

Article

# A New Spacetime Symmetry

Keith A. Fredericks<sup>1</sup> <sup>1</sup> Restframe Labs; keith@restframe.com, New York, NY 10019

Received: date; Accepted: date; Published: date

**Abstract:** Based on detection of elliptical particle tracks,  $\simeq 137^2 n^2$  bigger than Bohr-Sommerfeld electron orbits, indicating the possible detection of superluminal electrons masquerading as magnetic monopoles, new relations become accessible leading to: (i) a new set of seven elementary lengths; (ii) replacement of the usual motion (Lorentz) transformations by scale transformations between  $v^2 < c^2$  and  $v^2 > c^2$  frames; (iii) equivalence of charge between  $v^2 < c^2$  and  $v^2 > c^2$  frames based on the Dirac-Schwinger quantization condition; (iv) a relativistic foundation for the Dirac-Schwinger quantization condition; (v) a possible cause of charge quantization; and (vi) the prospect of symmetry in Maxwell's equations. If the elliptical particle tracks are viewed as a magnification of electron orbits, the effect is suggestive of a spacetime distortion such as those predicted in general relativistic theories.

**Keywords:** monopoles; tachyons; elliptical orbits; photographic emulsion; detection; Coulomb's law; Kepler orbits; hydrogen

## 1. Introduction

Recent experiments [1] provide missing pieces to the puzzle of faster-than-light particles and lead to a new framework allowing an entirely new approach to the theory. Specifically, our quantized elliptical particle tracks with sizes  $\simeq 137^2 n^2$  bigger than Bohr-Sommerfeld electron orbits are connected to the Dirac quantization condition, leading to elementary lengths mapped to extended relativity and ultimately to a new type of superluminal Lorentz transformation (SLT).

Two main approaches to a theory of faster-than-light particles, each focused on the transformation used for superluminal velocities, have been used [2]:

1. Assuming that standard Lorentz transformations can be used for superluminal velocities [3,4],  $\gamma = (1 - \beta)^{-1/2}$ , where  $\beta = v/c$  and  $\beta > 1$  and rest mass, proper length and proper time become imaginary, but this may not be important since it is not possible to measure these with  $v^2 < c^2$  observers [3,4].
2. Assuming that equivalent  $v^2 < c^2$  and  $v^2 > c^2$  frames exist and that it is possible to perform standard Lorentz transformations between them, the Lorentz factor becomes  $\gamma = (\beta - 1)^{-1/2}$ , where  $\beta = v/c$  and  $\beta > 1$  [5–7]. Here, frames, moving at superluminal relative velocities, partitioned at the speed of light, co-exist in our universe. Within each frame physicists observe the very same laws. This approach allows observers in  $v^2 > c^2$  frames, but, in four-dimensions, certain *imaginary quantities* enter the equations that cannot be measured [8,9].<sup>1 2</sup>

A new approach is presented here based on the first assumption of item 2. that equivalent  $v^2 < c^2$  and  $v^2 > c^2$  frames exist, but then, based on experiments, uses *scale transformations*, of the form  $\alpha^2 = (A^2 - 1)^{-1}$  where  $A = \ell/d$  and  $A > 1$  (see section 7.2.), to move between them. Using the analogy

<sup>1</sup> Recami and coworkers made significant advances, such as the (experimentally confirmed) X-shaped form of superluminal objects, despite the imaginary quantities, using the property of SLTs to invert the quadratic form sign. (see section 4).

<sup>2</sup> While we agree generally with the views expressed on superluminal worlds in Ref. [2] and imaginary quantities in Ref. [9], we disagree (see section 6) with the concept by the same author that, except for speed, superluminal electric charge would be equivalent to subluminal electric charge (see Refs. [9,10]).

of the bound electron with the bound monopole, this approach leads to a new symmetric framework where spacetime is partitioned by both the speed of light and a new length,  $d$  (see [subsection 7.1](#)) into two “worlds,” one with  $v^2 < c^2$  and  $\ell^2 < d^2$  and one with  $v^2 > c^2$  and  $\ell^2 > d^2$ . (See [Table 1](#)). Substituting a scale transformation for the standard SLT adds an entirely new physical interpretation to faster-than-light particles, and, as a side effect, avoids the imaginary quantities problem [1] (see [section subsection 7.5](#)) encountered in four-dimensional superluminal Lorentz transformations.

This approach systematically brings a simple single solution to problems associated with faster-than-light particles, magnetic monopoles, charge quantization and electric/magnetic symmetry.

**Table 1.** Symmetric Spacetime - Velocity and length mapped to classes of particles. The vertical interval between all values is  $\alpha$ . Type III particles) Tachyons with “charge”  $k_m g^2$ ,  $v^2 > c^2$ ,  $\ell^2 > d^2$  and coupling constant  $\alpha^{-1}$ . Type II particles) Luxons with velocity  $c$  corresponding to length  $d$ . Type I particles) Bradyons with “charge”  $k_e e^2$ ,  $v^2 < c^2$ ,  $\ell^2 < d^2$  and coupling constant,  $\alpha$ .

velocity (m/s)				length (m)		
III.	$7.72 \times 10^{14}$	$c\alpha^{-3}$	$d\alpha^{-3}$	$r_{0m}$	$1.86 \times 10^{-2}$	
	$5.63 \times 10^{12}$	$c\alpha^{-2}$	$d\alpha^{-2}$	$\lambda_{cm}$	$1.36 \times 10^{-4}$	
	$4.11 \times 10^{10}$	$v_{0m} \quad c\alpha^{-1}$	$d\alpha^{-1}$	$a_{0m}$	$9.93 \times 10^{-7}$	
II.	$2.99 \times 10^8$	$c \quad c\alpha^0$	$d\alpha^0$	$d$	$7.25 \times 10^{-9}$	
I.	$2.19 \times 10^6$	$v_{0e} \quad c\alpha^1$	$d\alpha^1$	$a_{0e}$	$5.29 \times 10^{-11}$	
	$1.60 \times 10^4$	$c\alpha^2$	$d\alpha^2$	$\lambda_{ce}$	$3.86 \times 10^{-13}$	
	$1.17 \times 10^2$	$c\alpha^3$	$d\alpha^3$	$r_{0e}$	$2.82 \times 10^{-15}$	

2. Experiments

In 1979, a technique was found using photographic emulsions that resulted in unusual particle tracks that had not been observed according to the scientific literature. The technique consists of “supplementary” uniform photon exposures on photographic emulsions. In total darkness or with the appropriate safelight, a relatively uniform exposure of photons is created from white LEDs of about 1200 mcd at a distance of 6cm from the surface of a lith emulsion such as Arista Ortho Litho 3.0 for a time of about 250 ms. Any additional imagewise exposures, during exposure to the ambient environment, as in a cosmic ray study, will be amplified using this technique. [1,11,12].

Microscopic examination of these tracks reveals structure consistent with particles traveling through emulsions (see elliptical track structure in Fig. 4 of Ref. [1]). A  $1/r^2$  central force is required to create elliptical particle tracks in any nuclear track detector. The elliptical tracks are excellent fits for ellipses [1]. Particle-like structure resulting from  $1/r^2$  central force strongly indicates that these detected tracks are caused by particles.

In 2002, Russian researchers reported similar tracks during experiments with electric explosion of metal wires and foils in water [13] and low-energy discharges in water [14]. It is clear, by comparison, that the same tracks were recorded with both supplementary photon exposures and electric discharges in these and other experiments [11,12].

In 2014, experiments were undertaken to determine if these particles could be affected by electric or magnetic fields [1]. Although no repeatable particle curvature resulted from applied electric or magnetic fields, *elliptical tracks* were found, often *in conjunction with decay events* [1]. The elliptical tracks add to the known properties [11] of the detected particle tracks. The elliptical tracks often occur at a point of decay of a primary track [1] (see [Figure 1](#) and [Figure 4](#)) and differ from the predominant detected tracks [11]. Since it was shown that curvature, due to applied electric or magnetic fields, has not been observed for the predominant tracks, it was conjectured [1] that the predominant tracks are neutral and possibly comprised of oppositely charged particles and that these neutral composite

particles may decay or split apart into separate charged particles. The separate charged particles may then become captured into elliptical orbits.

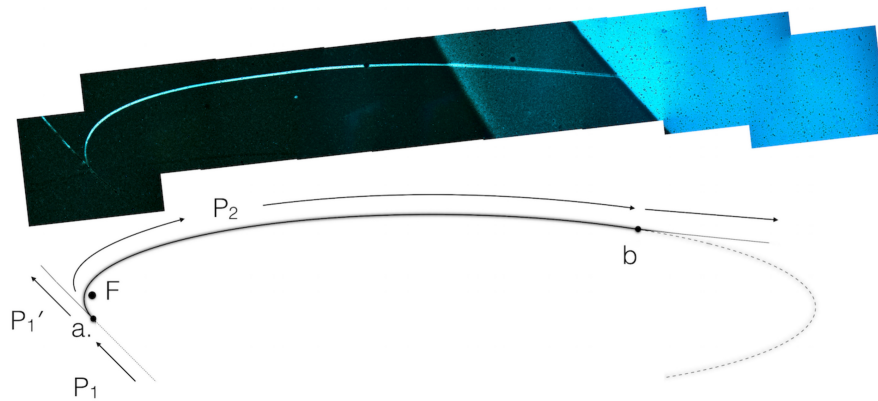


**Figure 1.** Track  $me$ ,  $n = 7$ . Top.) Semi-major axis size  $a = 2391.6 \pm 16.1 \mu m$ . Ten tile photomosaic at 160x. Bottom.) Capture into and escape from an elliptical orbit. 1.) initial particle,  $P_1$ , trajectory. 2.) at point a. particle decays into  $P_1'$ , continuing on initial trajectory and  $P_2$ , which is captured into an elliptical orbit. 3.) at point b. particle escapes from the elliptical orbit.

Out of a population of 750 exposures, 22 tracks with elliptical curvature were selected. The semi-major axis size of these tracks were measured to be  $\simeq 137^2 n^2$  larger than Bohr-Sommerfeld electron orbit semi-major axis sizes. In addition, the measured elliptical particle tracks were shown to be quantized (see Figure 2.).

### 3. Symmetric worlds

Dirac introduced the idea of electric charge quantization using the quantization condition [15] where  $g$ , magnetic charge is

$$g = \frac{ecn}{2\alpha} = ng_D, \quad n \in \mathbb{Z}, \quad (1)$$

where  $\alpha = k_e e^2 / \hbar c$ ,  $k_e \equiv (4\pi\epsilon_0)^{-1}$  and  $e$  is electric charge. This explanation of electric charge quantization due to monopoles continues to be the best yet found. With  $n = 2$ , Eq. (1) becomes equivalent to the  $n = 1$  Schwinger quantization condition [16]

$$g = \frac{ec}{\alpha} = 2g_D, \quad (2)$$

or, using shorthand,  $g = 2g_D$ .

From an analysis of the Dirac quantization condition, using Eq. (1) with  $n = 1$ , Datta [17] computed new elementary monopole lengths,  $a_{0m}$ ,  $\lambda_{cm}$  and  $r_{0m}$ , which are analogs of the Bohr radius,  $a_{0e}$ , the reduced Compton wavelength,  $\lambda_{ce}$ , (hereafter, Compton radius), and the classical electron radius,  $r_{0e}$ , and showed that a hierarchy,

$$a_{0m} < \lambda_{cm} < r_{0m} \quad (3)$$

exists as well as the usual hierarchy,

$$a_{0e} > \lambda_{ce} > r_{0e}. \quad (4)$$

In this analysis, Datta

- (i) used analogy with the electron for magnetic monopoles
- (ii) reasoned that hierarchy (3) makes monopoles inherently relativistic,
- (iii) expressed concern that the size of the classical monopole radius,  $r_{0m}$ , is so large that it would overlap with the anti-monopole with an orbital radius of  $a_{0m}$ , and

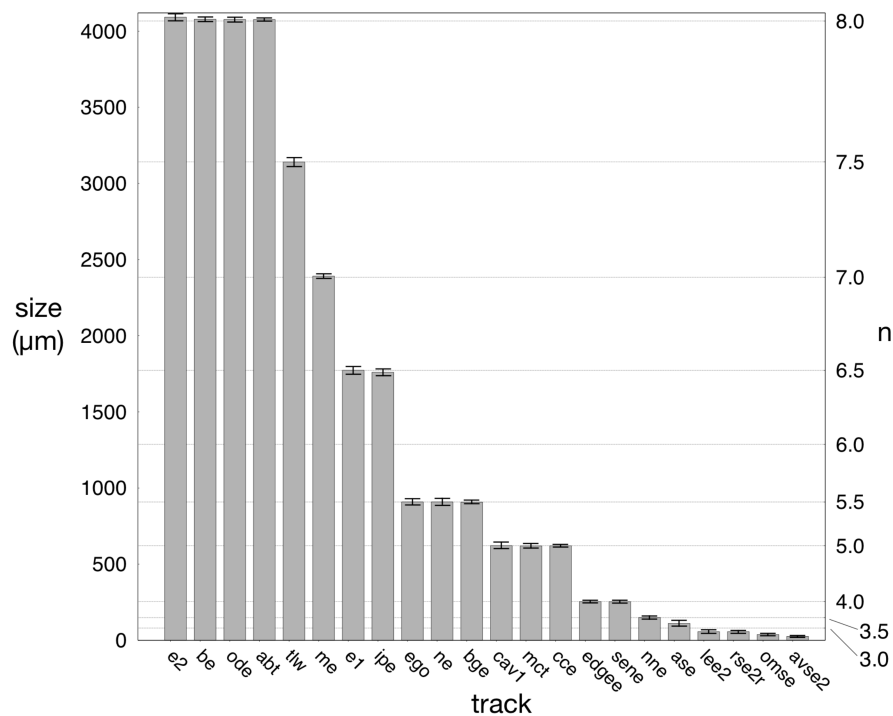


**Figure 2.** Quantized ellipse semi-major axis sizes. Ellipses between  $n = 8$  and  $n = 3.5$  are shown to be quantized as half integer values. Ellipses less than  $n = 3.5$  are quantized by quarter integer values. Error bars represent the combined standard uncertainty of the semi-major axis size.

- (iv) found that a pair of north and south monopoles in an *atom-like bound state* would require superluminal ground state orbital speeds as in Eq. (6).

Datta used the simple analogy of the bound monopole and the bound electron. For example, since the ground state velocity of the bound electron is

$$v_{0e} = k_e \frac{e^2}{\hbar} = c\alpha, \quad (5)$$

the ground state velocity of the bound monopole should be

$$v_{0m} = k_m \frac{g^2}{\hbar} = c/\alpha, \quad (6)$$

where ( $k_m \equiv \mu_0/4\pi$ ). Due to points (iii) and (iv) (i.e. Eq. (6)), Datta rejected monopoles as unphysical, ending his investigation.

These specific points will be considered later (see subsection 5.3), but the mapping of hierarchy (3) to faster-than-light monopoles in extended relativity warrants further investigation.

Continuing along these lines, first it is noted that using  $g = 2g_D$ , the coupling constant,  $\alpha$ , simply inverts with  $\beta$ . [18]

$$\alpha_{\text{EM}} = \begin{cases} \alpha, & \text{if } \beta < 1 \\ \alpha^{-1}, & \text{if } \beta > 1 \end{cases}.$$

Here the notation is used that  $\alpha_e = \alpha$  and  $\alpha_m = 1/\alpha$  where  $\alpha$  is the fine structure constant. Monopole mass can be found either by using the Compton radius of the monopole in terms of the Compton radius of the electron [18] or by using the analogy between the Bohr radius for the electron versus the

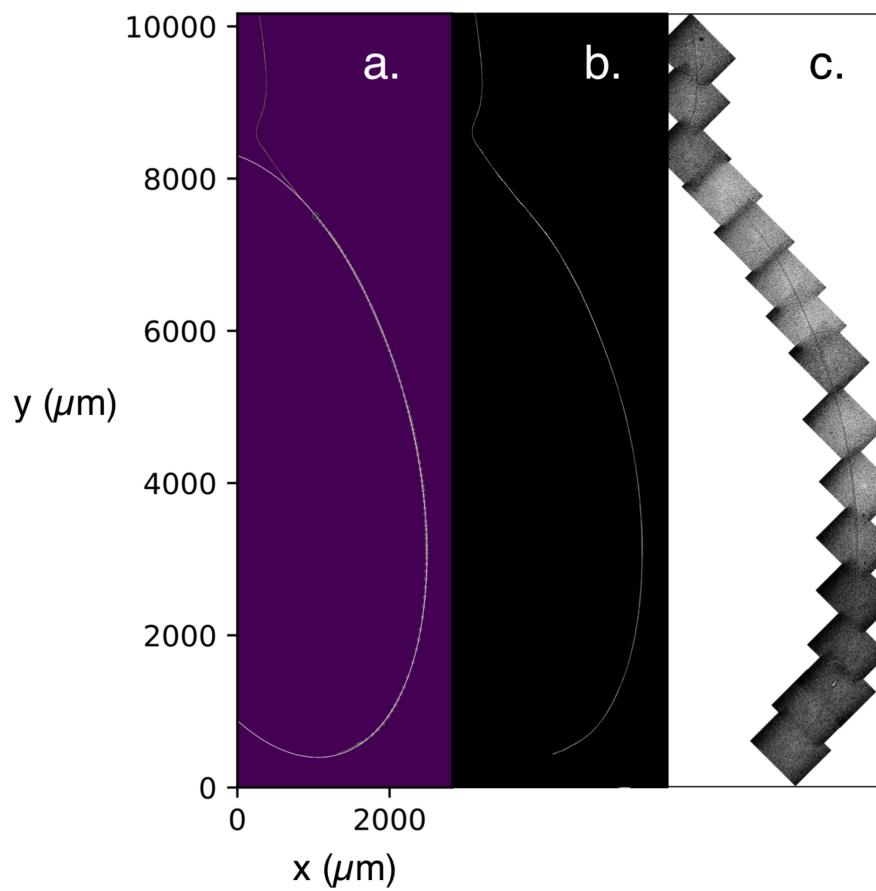


**Figure 3.** Track *be*. The semi-major axis size of  $a_m = 4078.6 \pm 14.6 \mu m$  is related to the semi-major axis size of an  $n = 8$  electron in hydrogen,  $a_e$  by  $a_m/137^2 n^2 \simeq a_e$ . a.) Least-squares fit of  $x, y$  track coordinates to ellipse overlayed on processed track image. b.) Track after image processing and background eradication. c.) Photo montage of track.

Bohr radius for the monopole using the  $1/\alpha^2$  relation derived from experiments [1]. Here the second approach is used. Using  $g = 2g_D$ , the ratio of the monopole Bohr radius to the electron Bohr radius is

$$\frac{a_{0m}}{a_{0e}} = \frac{1}{\alpha^2}. \quad (7)$$

Using the formula for Bohr radius,  $a_{0e} = \hbar/m_e c \alpha$ , the analogous  $a_{0m} = \hbar/m_m c \alpha_m$  and Eq. (7), monopole mass can be written as

$$m_m = \frac{m_e \alpha^3}{\alpha_m}, \quad (8)$$

and since  $\alpha_m = \alpha^{-1}$

$$m_m = m_e \alpha^4 = 1.45 \times 10^{-3} \text{eV}/c^2, \quad (9)$$

which leads to the fine structure constant,  $\alpha = (m_m/m_e)^{1/4}$ , as a mass ratio.

Using  $g = 2g_D$ , analogy with the electron, and monopole mass, Table 1. can be populated with values. The electron and monopole Bohr radii are equally offset from the length,  $d$ , corresponding to the speed of light,  $c$ , such that the monopole Bohr radius, is *scale symmetric* with the electron Bohr radius. A similar symmetric relation exists between the ground state orbital velocities and  $c$ . Thus  $c$  and  $d$  form the axis of symmetry for both Bohr radii, the ground state orbital velocities and hierarchies (3) and (4) [18] (see Table 1.).

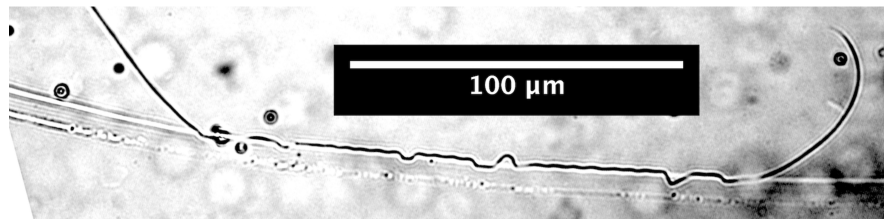


**Figure 4.** Track  $rse2$ ,  $n = 2.75$  showing elliptical track decay event. Photo at 400x.

Hierarchy (4) comprises a set of three elementary lengths each separated from the next by the fine structure constant,  $\alpha$ . With the identification of  $d = ct$  and hierarchy (3), The entire right side of Table 1. represents a new set of seven elementary lengths, each separated from the next by the fine structure constant.

#### 4. Extended relativity

After pioneering work by Jones [19], Parker [5] notably forwarded the idea of extending relativity to superluminal frames. He was also the first to suggest that when special relativity is extended to superluminal velocities, charged tachyons should be detected as magnetic monopoles by subluminal observers.

Baldo, *et.al* [20], Recami and Mignani, [21] and Recami [22] developed Parker's concepts [23–27]. Since faster-than-light electric charge, in this theory, brings into Maxwell's equations exactly what magnetic monopoles would (see section 8), subluminal monopoles were rejected and, using a symmetry argument, a magnetic charge of  $g = -ec$  was initially proposed in accordance with charge invariance (although later Schwinger quantization was favored). As a result, the coupling constant,  $\alpha$  took a singular value both above and below the speed of light. According to Recami, *et.al* slower-than-light monopoles do not exist.

The structure of extended relativity follows Bilaniuk, *et.al*'s [3] original classification of particles. That is:

- III. *tachyons* or  $v^2 > c^2$  particles. (from  $\tau\alpha\chi\iota\varsigma$ , swift),
- II. *luxons* or  $v = c$  particles (from Latin *lux*, light) and
- I. *braydons* or  $v^2 < c^2$  particles (from  $\beta\rho\alpha\delta\upsilon\varsigma$ , slow)

The symmetric spacetime in Table 1. maps one-to-one with the architecture of extended relativity [5,21,22], *i.e.* symmetric  $v^2 > c^2$  and  $v^2 < c^2$  worlds partitioned at  $c$ , the speed of light, symmetric  $\ell^2 > d^2$  and  $\ell^2 < d^2$  worlds partitioned at  $d$  (see subsection 7.1) or, more generally, type III and type I worlds partitioned by type II speed and length. Type III, type II, and type I will be used throughout in accordance with Table 1.

The central feature of extended relativity is the superluminal Lorentz transformation (SLT). The SLT shows what a type III object in a type III frame looks like to an observer in a type I frame and so connects observations of type I observers with observations of type III observers.

The collinear bi-dimensional  $(x, t)$  SLT works without problems, but, when extended to four dimensions,  $(x, y, z, t)$ , it leads to imaginary quantities [8,9] for certain measurements of  $v^2 > c^2$  (type III) objects and problems of how to interpret these physically. It is possible to use a six-dimensional spacetime for the SLT [28], but it may be difficult to physically interpret two additional time dimensions.

The standard collinear bi-dimensional SLT in its usual form will not transform the detected ellipse semi-major axis size into a Bohr-Sommerfeld ellipse semi-major axis size. That is

$$a_m^{(n)}(\gamma) \neq a_e^{(n)}, \quad \gamma = (\beta^2 - 1)^{-1/2}. \quad (10)$$

If the SLT is followed by an isotropic scale contraction of  $\alpha$  in accordance with the Schwinger quantization condition, the semi-major axis size corresponds to the Bohr-Sommerfeld semi-major axis



size, but the semi-minor axis size is only half the size it needs to be. The transformed ellipse is greatly distorted and does not correspond to a Bohr-Sommerfeld ellipse. With  $n = 8$  and  $l = 2$ ,

$$\begin{cases} a_m^{(n)}(\alpha\gamma) = a_e^{(n)} \\ b_m^{(n)}(\alpha) \neq b_e^{(n)} \end{cases} \quad (\gamma = (\beta^2 - 1)^{-1/2}, \quad \beta > 1), \quad (11)$$

and eccentricity,  $\mathcal{E} = 0.95 \rightarrow \mathcal{E}' = 0.99$ , markedly changes.

Using Recami's multidimensional approach, the SLT inverts the quadratic form sign [29] of an object and a bound superluminal electron detected as a monopole ellipse would be

$$0 \geq -\frac{x^2}{a_m^{(n)2}} + \frac{y^2}{b_m^{(n)2}} \geq -1, \quad (12)$$

consisting of the area between an on-central-axis conic section,

$$\frac{y^2}{b_m^{(n)2}} = \frac{x^2}{a_m^{(n)2}}, \quad (13)$$

and a hyperbola,

$$\frac{y^2}{b_m^{(n)2}} = \frac{x^2}{a_m^{(n)2}} - 1, \quad (14)$$

radically distorted from the original ellipse with eccentricity,  $\mathcal{E}' > 1$ , as shown in Figure 5.

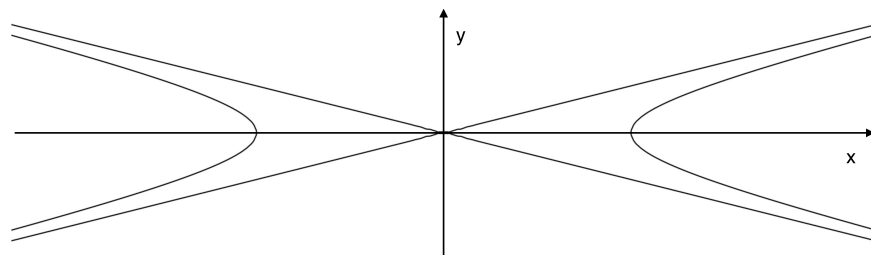


**Figure 5.** Recami type SLT of a theoretical  $n = 8$ ,  $l = 2$  monopole ellipse.

Objects such as these have been called *X-shaped waves*. An entire field of study and useful applications such as ultrasound scanning have resulted from the study of these X-shaped waves. Localized X-shaped waves have been shown to be superluminal [30].

The elliptical particle tracks we observe do not share the same semi-major axis size as their (presumed) subluminal counterparts, that is, the Bohr-Sommerfeld hydrogen semi-major axis sizes. They are larger by  $\alpha^{-2}$  and do not appear to be thoroughly distorted by stretching in one dimension.

The ratio of measured eccentricity,  $\mathcal{E}_\mu$  to Bohr-Sommerfeld eccentricity,  $\mathcal{E}_\tau$

$$\frac{\mathcal{E}_\mu}{\mathcal{E}_\tau} = \frac{(1 - b^2/a^2)^{1/2}}{n^{-1}(n^2 - \ell(\ell + 1))^{1/2}}, \quad (15)$$

as a ratio of averages over the 22 measured track values,  $\langle \mathcal{E}_\mu \rangle / \langle \mathcal{E}_\tau \rangle = 0.99$ , and measured eccentricity corresponds well to Bohr-Sommerfeld electron orbit eccentricity. This implies that the superluminal transformation, for this restricted case of bound particles, should be a scale transformation.

Since measured eccentricity corresponds to pure Bohr-Sommerfeld eccentricity, then, due to the  $\alpha^{-2}$  size change, the transformation of ellipses in general needs to be an isotropic *scale* transformation instead of a translation along one axis.

## 5. The Coulomb flip

Coulomb's law for magnetism and electricity is

$$F_m = k_m \frac{g^2}{r_m^2} \quad \text{and} \quad F_e = k_e \frac{e^2}{r_e^2}.$$

The force difference between magnetism and electricity using  $g = 2g_D$ ,  $r_e = a_{0e}$  and  $r_m = a_{0m}$  is

$$\frac{F_m}{F_e} = \frac{k_m g^2 / a_{0m}^2}{k_e e^2 / a_{0e}^2} = \alpha^{-2} \simeq 137. \quad (16)$$

Since detected ellipses are the same shape but  $137^2 n^2$  different in size from Bohr-Sommerfeld electron orbits, the most direct explanation would be that these are Bohr-Sommerfeld (type III) monopole orbits and the required transformation is identical to the force ratio, from Eq. (16) between magnetic and electric force strengths, which is a scale ratio, dilatation ( $\alpha^{-2}$ ) or contraction ( $\alpha^2$ ), which can be called the *Coulomb flip*.

The magnetic and electric Bohr-Sommerfeld Kepler ellipses are completely analogous and scale symmetric with respect to the speed of light,  $c$  and the length,  $d$ . Using  $g = 2g_D$ , the Kepler period for an electron in hydrogen and the “monopole” in a magnetic hydrogen analog,

$$t_m^{(n)} = \frac{2\pi a_{0m} n^3}{v_{0m}} = \frac{2\pi a_{0e} n^3}{v_{0e}} = t_e^{(n)}, \quad (17)$$

are equal.

The one-dimensional basis Coulomb flip contractions from type III to type I are

$$\text{coupling constant} \quad \alpha_{EM} : \quad \alpha_m (\alpha^2) = \alpha_e, \quad (18a)$$

$$\text{Bohr radius} \quad a_0 : \quad a_{0m} (\alpha^2) = a_{0e}, \quad (18b)$$

$$\text{ground state } v \quad v_0 : \quad \alpha_m c (\alpha^2) = \alpha_e c, \quad (18c)$$

$$\text{charge} \quad q_0^2 : \quad k_m g^2 (\alpha^2) = k_e e^2. \quad (18d)$$

Combining the basis transformations, Eqs. (18b), (18c), and (18d) and assuming  $\hbar$  is Coulomb flip invariant, transformations between type III and type I frames for time, momentum, binding energy and mass are

$$t_m = \frac{2\pi a_{0m}}{\alpha_m c} \xrightarrow{(\alpha^2)} \frac{2\pi a_{0e}}{\alpha_e c} = t_e \quad (19a)$$

$$p_m = \frac{\hbar}{a_{0m}} \xrightarrow{(\alpha^2)} \frac{\hbar}{a_{0e}} = p_e \quad (19b)$$

$$E_m = -\frac{k_m g^2}{2a_{0m}} \xrightarrow{(\alpha^2)} -\frac{k_e e^2}{2a_{0e}} = E_e \quad (19c)$$

$$m_m = \frac{\hbar}{a_{0m} \alpha_m c} \xrightarrow{(\alpha^2 \alpha^2)} \frac{\hbar}{a_{0e} \alpha_e c} = m_e \quad (19d)$$

and the “monopole” and electron properties can be transformed into one another using Coulomb flips with  $g = 2g_D$ . Time, in Eq. (19a) and energy in Eq. (19c) are invariant (in the ground state).



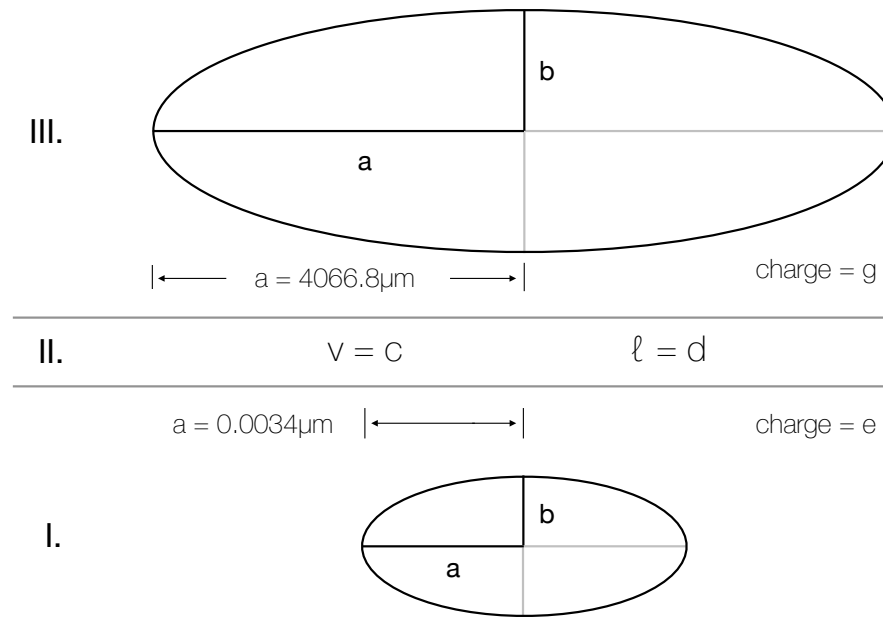


**Figure 6.** How a type I observer sees a type I electron orbit and an  $n = 8, l = 2$  type III “monopole” orbit. The type III orbit is transformed to the type I orbit using the 2-dimensional Coulomb flip Eq. (20) (Not to scale).

### 5.1. 2D Coulomb flip

The 2-dimensional Coulomb flip scales (contracts) the parametric equation of the “monopole” ellipse (upper ellipse in Figure 6), by the factor  $\alpha^2/n^2$ ,

$$\begin{bmatrix} x \\ y \end{bmatrix} = \frac{\alpha^2}{n^2} \begin{bmatrix} a_m^{(n)} \cos\theta \\ b_m^{(n)} \sin\theta \end{bmatrix} = \begin{bmatrix} a_e^{(n)} \cos\theta \\ b_e^{(n)} \sin\theta \end{bmatrix}, \quad (20)$$

where  $0 \leq \theta \leq 2\pi$ , to the electron ellipse (lower ellipse in Figure 6).

### 5.2. 3D Coulomb flip

The parametric equation to contract a sphere of  $r = a_{0m}$  to  $r = a_{0e}$  using a scale factor of  $\alpha^2$  is

$$\begin{bmatrix} x \\ y \\ z \end{bmatrix} = a_{0m} \alpha^2 \begin{bmatrix} \sin\theta \cos\varphi \\ \sin\theta \sin\varphi \\ \cos\theta \end{bmatrix} = a_{0e} \begin{bmatrix} \sin\theta \cos\varphi \\ \sin\theta \sin\varphi \\ \cos\theta \end{bmatrix}, \quad (21)$$

where  $0 \leq \theta \leq 2\pi$  and  $0 \leq \varphi \leq \pi$ .

### 5.3. Consequences

Returning to hierarchies (3) and (4), type III observers will see what we refer to as hierarchy (3) as their normal electric hierarchy (4). In their home frame, type I observers and particles will recognize the type III electric charge as a magnetic charge. The mirror hierarchies map one-to-one with extended relativity, except that we are dealing with lengths (scale transformations) instead of velocities (Lorentz transformations).

Datta’s points (ii) and (iii) above are nullified if hierarchy (3) is a type I to type III transformation of hierarchy (4) (that is, hierarchy (3) would just be the normal hierarchy (4) to type III observers). Datta’s point (iv) is therefore relevant and could indicate the unrealized discovery of type III lengths and symmetric spacetime.

## 6. Transformation of charge

Even though a type III particle's observed (by a type I observer) charge state is magnetic, it *should* possess exactly the same amount of charge in its own rest frame where the charge state is electric. This is to say that type III electric charge is observed by normal type I observers to be magnetic charge and that type I magnetic charge does not exist [23,24].

As noted earlier, equivalence of charge along with considerations of special relativity motivated Recami, *et.al.* initially to propose  $g = -ec$  and deviate from the Dirac-Schwinger quantization condition (although later Schwinger quantization was favored). In light of  $g = 2g_D$  it is possible to reconsider this issue.

The basis Coulomb flip for charge in Eq. (18d) shows that, after transformation, the magnetic charge is equivalent to the electric charge in a type III frame observed from a type I frame.

Solving for  $g$  in (18d) with  $k_m/k_e = 1/c^2$  yields  $g = ec/\alpha$ , which is the Schwinger quantization condition. So the Coulomb flip for charge is just the Schwinger quantization condition.

## 7. Relativistic transformations

In Table 1. on the length side, the Bohr, Compton and classical electron radii clearly represent the radii of spheres, *i.e.* the basis for a three-dimensional or spatial scale. This stands in contrast to the one-dimensional velocity scale on the left side of the table upon which special relativity is based.

### 7.1. The length $d$

The length  $d$  emerged as it became evident that hierarchies (3) and (4) were equally separated from a central length by  $\alpha$ . As can be seen in Table 1, the length  $d$  corresponds to  $c$ . Many computations can use  $d$  analogously to  $c$ . There is a direct correspondence between the transformation of velocities and the transformation of lengths between type III and type I frames as in

$$v_{0m} = c^2/v_{0e}, \quad (22a)$$

$$a_{0m} = d^2/a_{0e}. \quad (22b)$$

Monopole mass can be computed again (as in Eqs. (8) and (9)) using the relations for the Bohr radius,  $a_{0e} = \hbar/m_e c \alpha$  and the analogous  $a_{0m} = \hbar/m_m c \alpha^{-1}$ , but this time using the relation (22b) and substituting  $d^2/a_{0e}$  for  $a_{0m}$ , which results in

$$\frac{d^2 m_e c \alpha}{\hbar} = \frac{\hbar}{m_m c / \alpha}. \quad (23)$$

Solving for "monopole" mass

$$m_m = \frac{\hbar^2}{d^2 c^2 m_e} = 1.45 \times 10^{-3} \text{eV}/c^2. \quad (24)$$

For now we simply note that  $d$  is totally analogous with  $c$ .

### 7.2. Length transformations

With the new elementary length  $d$ , it becomes possible to represent relativistic transformations equivalently using either length or velocity. Where  $v$  is velocity on the left side of Table 1. and  $\ell$  is length on the right side of Table 1.,  $v/c = \ell/d$  and so we can write

$$\beta = A, \quad (25)$$

where  $\beta = v/c$  and  $A = \ell/d$ . In addition, since the *superluminal* Lorentz factor is

$$\gamma = (\beta^2 - 1)^{-1/2}, \quad (\beta > 1), \quad (26)$$

we can write the equivalent

$$\alpha = (A^2 - 1)^{-1/2}, \quad (A > 1). \quad (27)$$

Since  $A = \beta$ , the length-based forms can be substituted for the velocity-based forms in relativistic computations.

Because the lengths are three-dimensional spatial radii as opposed to a one-dimensional velocity vector, this affords a natural way to differentiate between motion-based velocity transformations and the length-based scale transformations. Using this notation it is possible to show the  $\alpha^2$  scale transformation (the Coulomb flip) as a relativistic transformation

$$\alpha^2 = (A^2 - 1)^{-1}. \quad (28)$$

Eq. (28) can be seen as the relativistic factor between type I and type III worlds, replacing Eq. (26) of the superluminal Lorentz transformation. That is, *intra-frame* transformations should use standard Lorentz transformations, i.e.  $\gamma = (1 - \beta^2)^{-1/2}$ , and *inter-frame* transformations could use Eq. (28), the Coulomb flip.

### 7.3. Relativistic expressions

The relation of the two symmetric Compton radii, from Table 1., converted to masses using  $\chi_m^{-1}(\hbar c/e)$  and  $\chi_e^{-1}(\hbar c/e)$ , are at once seen as the electron and “monopole” masses and, in terms of relativity, if the electron mass  $m_e = m_0$ , i.e. the rest mass in our type I frame, then the “monopole” mass,  $m_m = m'$ , is the “scale relativistic mass” as shown in Eq. (19d). The relativistic expression becomes

$$m_m = \frac{m_e}{(A^2 - 1)^2}. \quad (29)$$

The same thing can be done for each of the Eqs. (18) and (19), substituting  $(A^2 - 1)^{-1}$  for  $\alpha^2$ .

### 7.4. The quantization condition

In section 6 it was shown that the Schwinger quantization condition constitutes the transformation of charge between type I and type III frames. The Schwinger quantization condition  $g = ec/\alpha$  is also a Coulomb flip and can be represented as

$$g = \frac{ec}{(A^2 - 1)^{1/2}}, \quad (30)$$

adding a relativistic interpretation to this quantum relation.

### 7.5. Imaginary quantities

The imaginary quantities problem originates when two observers,  $O$  in the type I world,  $S$  and  $O'$  in the type III world,  $S'$  try to make measurements in each other's frames of the length of a rod held orthogonal to the direction of the superluminal relative velocity of the frames. If  $O$ , using a light pulse, tries to make a measurement on such a rod held by  $O'$ , the measurement cannot be made because the light pulse never catches up to the end of the rod [9]. Likewise if  $x$  is the axis of the superluminal boost and  $O$  uses an SLT to compute the rod length orthogonal to the boost direction in  $S'$ , it is found that the orthogonal quantities,  $y'_0 = iy_0$  and  $z'_0 = iz_0$ , become imaginary [8]. The reason imaginary quantities enter the computation is due to the superluminal relative velocity of frames.

We have shown that it is possible to *choose* to transform between  $S'$  and  $S$  using the Coulomb flip instead of an SLT. For the Coulomb flip, superluminal relative motion occurs as a result of an

observed scale difference between equivalent frames rather than a superluminal relative velocity between equivalent frames. The following sketches compare the SLT with the Coulomb flip.

### 7.5.1. SLT - frames with superluminal relative velocity

$O'$  records a three-dimensional reflection hologram of a hydrogen atom, at rest in  $S'$ , and sees that the hologram of the atom shows a spherical structure.  $O$  is able to detect the hologram created by  $O'$  and the hologram is seen by  $O$  as a structure bounded by a two-sheeted hyperboloid of revolution, asymptotic to a double cone [29].

In the analysis,  $O$  suspects that a superluminal object was just observed and describes frames  $(S, S')$  as

$$c^2t^2 - x^2 - y^2 - z^2 = -(c^2t'^2 - x'^2 - y'^2 - z'^2), \quad (31)$$

and uses an SLT along  $x$  collinear with  $x'$ ,

$$\begin{cases} x = \pm\gamma(x' + vt'), \\ t = \pm\gamma(t' + vc^{-2}x'), \\ y = \pm iy', \\ z = \pm iz', \\ \gamma = (\beta^2 - 1)^{-1/2}, \end{cases}$$

showing that the quantities  $y$  and  $z$  are imaginary [9,31] and, if a superluminal object was observed, were present in the observation.

### 7.5.2. Coulomb flip - static spherically symmetric frames

$O'$  records a three-dimensional reflection hologram of a hydrogen atom, at rest in  $S'$ , and sees that the hologram of the atom shows a spherical structure.  $O$  is able to detect the hologram created by  $O'$  and the hologram is seen as a sphere by  $O$ , which is measured to be about  $137^2$  bigger than a Bohr-Sommerfeld hydrogen atom. In the analysis,  $O$  suspects that a superluminal object was just observed and describes two equivalent static spherically symmetric frames,  $(S, S')$ , with co-located origins as

$$-dt^2 + dr^2 + r^2d\Omega^2 = -dt'^2 + dr'^2 + r'^2d\Omega^2, \quad (32)$$

where  $d\Omega^2 \equiv d\theta^2 + \sin^2\theta d\phi^2$ , and uses a Coulomb flip between  $S$  and  $S'$  defined by

$$\begin{cases} dr = dr'\alpha^2, \\ dt = dt', \\ \alpha^2 = A^2 - 1, A = \ell/d, \end{cases} \quad (33)$$

and sees that the transformation between  $S'$  and  $S$  is due to a scale change between frames, leaving all quantities real for this observation.

Imaginary quantities enter the computation for an SLT while all quantities of a Coulomb flip remain real.

## 8. Maxwell's equations

As has been mentioned previously, it is possible to recover symmetry in Maxwell's equations since type III particles with electric charge constitute magnetic charge in the equations. In extended relativity, Maxwell's equations for type I and type III particles, take a form [23,26]

$$\begin{aligned}\nabla \cdot D &= \rho_e(\text{I}) \\ \nabla \cdot B &= -\rho_m(\text{III}) \\ \nabla \times E &= j_m(\text{III}) - \frac{\partial B}{\partial t} \\ \nabla \times H &= j_e(\text{I}) + \frac{\partial D}{\partial t}\end{aligned}$$

where I = type I frame and III = type III frame.

## 9. The $\alpha^{-2}x$ lens

If a type I observer peers into a type III frame, detects type III electrons and then transforms the detection using a Coulomb flip, this is equivalent to an  $\alpha^{-2}x$  magnification since type III electrons are by definition the same as type I electrons. This would mean that observing type III objects could provide a portal of magnification, analogous to gravitational lensing, into our own world such that *e.g.* electron orbits could be examined at  $\alpha^{-2}x$  ( $\sim 1.88 \times 10^4x$ ) magnification.

## 10. Discussion

Due to the sizes of detected elliptical particle tracks, the particles that created these tracks were found to have properties consistent with faster-than-light particles in an extended relativity theory. But the eccentricity of the detected ellipses, compared with Bohr-Sommerfeld ellipses, required the transformation between  $v^2 < c^2$  and  $v^2 > c^2$  frames to be an isotropic scale transformation rather than the SLT commonly used in extended relativity.

A symmetric world is defined in Table 1 including both length and velocity-based values above and below a border delineated by  $c$  and  $d$  and generalizes these three regions into type I, type II, and type III frames.

To get between type I and type III frames, extended relativity models use Lorentz velocity transformations, represented by the left (velocity) side of Table 1. Based on the right (length) side of this diagram, an alternative is considered to use scale transformations called Coulomb flips to transform between type I bound electron and type III bound "monopole" states. A number of Coulomb flips are shown in Eqs. (18) (19), (20) and (21).

This correspondence between the velocity-based and length-based transformations and the subsequent use of scale transformations brings into question the physical interpretation of the transformations. If the radius-based scale transformation is chosen, frames in extended relativity can be separated by scale rather than superluminal velocities *and yet support superluminal relative velocities*.

If electrons from a type III frame were detected as magnetic charges in a type I frame, then Dirac's concept for the origin of charge quantization, defined as the interaction between magnetic charges and electrons *should* automatically become evidence for electromagnetic interaction between type I and type III worlds. A further implication of detecting electrons from a type III frame is to resolve the asymmetry between electricity and magnetism, thereby bringing symmetry to Maxwell's equations.

Charge in a type III frame can be transformed to charge in a type I frame by means of a Coulomb flip. In addition, the transformation of charge from a type III to a type I frame can be represented as a relativistic transformation based on the Schwinger quantization condition. So the foundation for magnetic monopoles can be shown to be electric charge in a type III frame, which is connected with electric charge in a type I frame by a relativistic transformation. Recami and Mignani had shown this earlier by SLTs of  $E$  and  $H$  fields (see *e.g.* [21,22])

## 11. Conclusion

Experimental results are discussed where quantized elliptical particle tracks  $137^2 n^2$  larger than Bohr-Sommerfeld electron orbits were detected [1]. Analysis indicated consistency between these particles and the properties expected of tachyon monopoles in extended relativity theories.

This led to the reexamination of a key discovery by Datta of superluminality resulting from the Dirac quantization condition, originally excluded [17], but here recovered [18]. This, in turn led to a symmetric spacetime structure in Table 1 forming a *basis* for theories of extended relativity.

Combining the experimental results with the symmetric spacetime structure leads to a new alternative isotropic scale transformation between type I and type III frames called the Coulomb flip.

The results presented here lead to possible solutions for problems of magnetic monopoles, charge quantization, equivalence of charge between type I and type III frames, imaginary quantities in four dimensional SLTs and electric/magnetic symmetry in Maxwell's equations.

Since transformations of observations of type III particles constitutes the observation of a scale change, it is possible that simply observing type III particles is analogous to a gravitational lens, but with higher magnification.

Further experiments are required to study the elliptical tracks in greater detail using thicker (10 - 100  $\mu\text{m}$ ) nuclear track emulsions with higher (> 80%) AgBr/gelatin ratios.

**Funding:** This research received no external funding.

**Acknowledgments:** The author gratefully acknowledges stimulating discussions and assistance of Erasmo Recami without whose extensive body of work this would not have been possible.

**Conflicts of Interest:** The author declares no conflict of interest.

## Abbreviations

The following abbreviations are used in this manuscript:

SLT    superluminal Lorentz transformation

## References

1. Fredericks, K.A. Elliptical Tracks: Evidence for Superluminal Electrons? Preprints, 2019070181, doi:10.20944/preprints201907.0181.v1.
2. Corben, H.C. Thought experiments at superluminal relative velocities. *Int. J. Theor. Phys.* **1976**, *15*, 703–712. doi:10.1007/BF01807318.
3. Bilaniuk, O.M.P.; Deshpande, V.K.; Sudarshan, E.C.G. "Meta" Relativity. *Am. J. Phys.* **1962**, *30*, 718.
4. Feinberg, G. Possibility of Faster-Than-Light Particles. *Phys. Rev.* **1967**, *159*, 1089–1105. doi:10.1103/PhysRev.159.1089.
5. Parker, L. Faster-Than-Light Intertial Frames and Tachyons. *Phys. Rev.* **1969**, *188*, 2287–2292. doi:10.1103/PhysRev.188.2287.
6. Recami, E.; Mignani, R. More about Lorentz transformations and tachyons: answer to the comments by Ramachandran, Tagare and Kolaskar. *Lett. Nuovo Cim.* **1972**, *4*, 144–152. doi:10.1007/BF02907136.
7. Goldoni, R. Faster-than-light inertial frames, interacting tachyons and tadpoles. *Lett. Nuovo Cim.* **1972**, *552*, 495–502. [*Lett. Nuovo Cim.* 5,495(1972)], doi:10.1007/BF02785903.
8. Recami, E.; Maccarrone, G.D. Solving the « imaginary quantities » problem in superluminal lorentz transformations. *Lett. Nuovo Cim.* (1971-1985) **1980**, *28*, 151–157. doi:10.1007/BF02772921.
9. Corben, H.C. Imaginary quantities in superluminal Lorentz transformations. *Lett. Nuovo Cim.* (1971-1985) **1974**, *11*, 533–536. doi:10.1007/BF02902720.
10. Corben, H.C. Tachyon matter and complex physical variables. *Nuovo Cim. A* **1975**, *29*, 415–426. doi:10.1007/BF02735713.
11. Fredericks, K.A. Possible detection of tachyon monopoles in photographic emulsions. *Eng. Phys.* **2013**, *6*, 15–45. doi:10.5281/zenodo.1133128.

12. Fredericks, K.A. Possibility of Tachyon Monopoles Detected in Photographic Emulsions. *J. Condens. Mat. Nucl. Sci.* **2015**, *15*, 203–230. doi:10.5281/zenodo.1133134.
13. Urutskoev, L.I.; Liksonov, V.I.; Tsinoev, V.G. Observation of transformation of chemical elements during electric discharge. *Ann. Fond. L. de Broglie* **2002**, *27*, 701, [arXiv:physics/0101089].
14. Ivoilov, N.G. Low energy generation of “strange radiation”. *Ann. Fond. L. de Broglie* **2006**, *31*, 115.
15. Dirac, P.A.M. Quantised Singularities in the Electromagnetic Field. *Proc. Royal Soc. A* **1931**, *133*, 60–72. doi:10.1098/rspa.1931.0130.
16. Schwinger, J. Magnetic Charge and Quantum Field Theory. *Phys. Rev.* **1966**, *144*, 1087–1093. doi:10.1103/PhysRev.144.1087.
17. Datta, T. The fine-structure constant, magnetic monopoles and dirac charge quantization condition. *Lett. Nuovo Cim.* **1983**, *37*, 51–54. doi:10.1007/BF02818083.
18. Fredericks, K.A. Monopole mass from fundamental lengths. *Phys. Essays* **2017**, *30*, 269–271. doi:10.4006/0836-1398-30.3.269.
19. Jones, R.T. Conformal coordinates associated with space-like motions. *J. Frankl. Inst.* **1963**, *275*, 1 – 12. doi:https://doi.org/10.1016/0016-0032(63)90616-1.
20. Baldo, M.; Fonte, G.; Recami, E. About charged tachyons. *Lett. Nuovo Cim. (1969-1970)* **1970**, *4*, 241–247. doi:10.1007/BF02755682.
21. Recami, E.; Mignani, R. Classical theory of tachyons (special relativity extended to superluminal frames and objects). *Riv. Nuovo Cim.* **1974**, *4*, 209–290. doi:10.1007/BF02747655.
22. Recami, E. Classical tachyons and possible applications. *Riv. Nuovo Cim.* **1986**, *9*, 1–178. doi:10.1007/BF02724327.
23. Mignani, R.; Recami, E. Magnetic monopoles and tachyons. *Lett. Nuovo Cim.* **1974**, *9*, 367–372. doi:10.1007/BF02756328.
24. Recami, E.; Mignani, R. Do magnetic monopoles exist? Considerations for theory and experiments. *Lett. Nuovo Cim.* **1974**, *9*, 479–482. doi:10.1007/BF02819915.
25. Mignani, R.; Recami, E. Possible experimental behaviour of tachyon monopoles. *Lett. Nuovo Cim.* **1974**, *11*, 417–420. doi:10.1007/BF02827275.
26. Recami, E.; Mignani, R. Magnetic monopoles and tachyons in special relativity. *Phys. Lett. B* **1976**, *62*, 41 – 43. doi:10.1016/0370-2693(76)90042-3.
27. Recami, E.; Mignani, R. A new approach and experimental outlook on magnetic monopoles. In *The Uncertainty Principle and Foundations Of Quantum Mechanics*; Price, W.C.; Chissick, S.S., Eds.; Wiley, London, 1977; pp. 321–324.
28. Cole, E.A.B. Superluminal transformations using either complex space-time or real space-time symmetry. *Il Nuovo Cim. A (1965-1970)* **1977**, *40*, 171–180. doi:10.1007/BF02776784.
29. Barut, A.; Maccarrone, G.; Recami, E. On the shape of tachyons. *Nuovo Cim. A* **1982**, *71*, 509–533. doi:10.1007/BF02770989.
30. Recami, E.; Zamboni-Rached, M. Chapter 4 Localized Waves: A Review. In *Advances in IMAGING AND ELECTRON PHYSICS*; Hawkes, P.W., Ed.; Elsevier, 2009; Vol. 156, *Advances in Imaging and Electron Physics*, pp. 235 – 353. doi:https://doi.org/10.1016/S1076-5670(08)01404-3.
31. Maccarrone, G.D.; Recami, E. Revisiting the superluminal Lorentz transformations and their group-theoretical properties. *Lett. Nuovo Cim.* **1982**, *34*, 251–256. doi:10.1007/BF02817120.